Time-of-Flight Depth Camera Motion Blur Detection and Deblurring

Seungkyu Lee, *Member, IEEE*

***Abstract*—Recently, many consumer time-of-flight depth cameras have been introduced that provide direct 3-D geometry measurement of real world objects in real-time. However, these cameras suffer from motion blur artifact when there is any movement of camera or target object in the scene causing serious geometry measurement distortions. Unlike other noises, depth camera motion blur is difficult to eliminate using any existing image processing method due to the unique principle of time-of-flight depth calculation. In this letter, we propose a novel depth motion blur detection and deblurring method that can be applied for any ToF depth sensor. Our method utilizes the relations between different phase offsets observed at multiple time slots in ToF sensor. Experimental results show that the proposed method successfully detects motion blur regions and accurately eliminates them with minimal computational cost in real time.**

***Index Terms*—Deblurring, depth, motion blur, time-of-flight.**

I. Introduction

TIME-OF-FLIGHT (ToF) sensor produces miscalculated depth values when they observe a moving object. This motion blur is serious error for accurate 3-D data acquisition. With an appropriate model of the situation and time-of-flight sensing principle, we can infer correct depth values from the miscalculations understanding the underlying mechanism of the motion blur. Different from passive photometry sensors that collectively count the number of photons arriving at each pixel, active sensors such as time-of-flight camera count the relative amount of photons at multiple time instances. These sensors investigate the flight time of emitted and reflected light source to calculate the distance. Phase offset between emitted and reflected infrared waves can tell the distance from camera to target object. Distance image, as a result, is an integration of phase offset values from all sensor pixels.

When there is any movement of an object or camera, the phase offset observed at corresponding sensor pixel changes causing *Phase Mixing* within an integration time. The phase mixing causes miscalculation of depth value based on multiple reflected IR waves having different phase offsets. As a result, the phase mixing within a photon integration time produces motion blur in the result depth image. Motion blur region in a depth image is the group of pixels observing phase mixing. Shorter integration time will alleviate this artifact, however, it is not always preferable solution because it also reduces the amount of photons collected at each sensor pixel decreasing signal to noise ratio. Post processing methods after depth image acquisition show limited performance and they are computationally expensive [1].

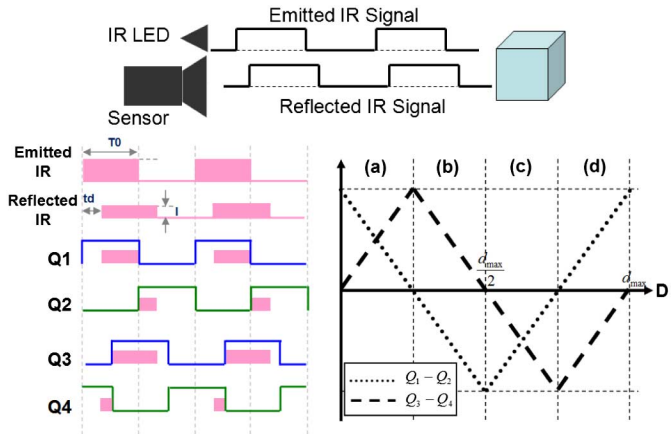

Fig. 1. ToF depth sensing principle based on emitted IR signal with fixed wavelength. Depth can be calculated by measuring the phase offset between emitted and reflected IR signals. $Q_1 \sim Q_4$ represent the amount of electric charge values collected by multiple control signals $C_1 \sim C_4$ respectively.

Unlike conventional color motion blur showing smooth transition over different colors [2], depth motion blur frequently shows unusual peaks in depth value at the transition region [3]. This is because the ToF camera uses multiple electric charge values measured at different time slots to calculate single depth value (Fig. 1). ToF depth camera emits IR signals of fixed wavelength and measures the phase offset between the emitted and reflected IR signals to obtain the depth from the camera to objects. This unique imaging principle affects the different characteristics of depth image motion blur pixels.

Hussmann *et al.* [4] analyze a motion blur effect on a conveyor belt where only single direction of rigid object motion artifact will be observed. Lottner *et al.* [5] propose a specific internal sensor control signal based blur detection method that is restricted in extending to general users and recovering the blur pixels. Lindner *et al.* [6] try to model the ToF motion blur to compensate the artifact, however, they introduce a simple blur model which can only work on some simple blur cases. Schmidt and Jahne [7] introduce motion blur reduction method by analyzing the temporal variation of each depth image pixel. Lee *et al.* [3] introduce the principle of ToF depth motion blur artifact and propose simple blur region detection method. In order to reduce the blur pixel they use normal neighbour pixels. Lee *et al.* [1] propose a depth image post-processing method for blur

Manuscript received December 09, 2013; revised March 04, 2014; accepted March 06, 2014. Date of publication March 18, 2014; date of current version March 27, 2014. This work was supported by Kyung Hee University in 2013 under Grant KHU-20130684. The associate editor coordinating the review of this manuscript and approving it for publication was Prof. Weisi Lin.

The author is with the Department of Computer Engineering, Kyung Hee University, Seoul, Korea (e-mail: seungkyu74@gmail.com).

Color versions of one or more of the figures in this paper are available online at http://ieeexplore.ieee.org.

Digital Object Identifier 10.1109/LSP.2014.2312384

detection which has limitations in real-time implementation and deblurring performance.

In this letter, 1) we investigate the underlying mechanism of depth motion blur based on the principle of ToF sensor. We analyze how ToF depth motion blur occurs in natural environments. 2) And we propose a fast, efficient and accurate pixel-wise motion blur elimination method that is free from any loss of image details and expects no additional memory spending minimal processing time. In Section II, we study underlying principle of ToF depth calculation. In Section III, motion blur is investigated in terms of phase mixing and blur region detection method is proposed. Finally, our deblurring method is proposed and experimentally evaluated in Section IV and V respectively.

II. Depth Sensing Principle

Fig. 1 illustrates a principle of ToF depth sensing. An IR signal is emitted to target object and the sensor accepts reflected IR signal. In order to measure the phase offsets between the emitted and reflected IR signals, ToF sensors have multiple control signals ($C_1 \sim C_4$) that are alternately turned on and off. With the assumptions that our emitted IR signal is square wave and control signals $C_1 \sim C_4$ collect electric charge values $Q_1 \sim Q_4$, the phase offset is calculated by the relation between $Q_1 \sim Q_4$. Four phase control signals $C_1 \sim C_4$ works with 90 degree of phase offset to each other. They collect electric charge values when the signal is in high voltage status. These four electric charge values $Q_1 \sim Q_4$ are used to calculate depth using the following formulation [8]. In this letter, we assume that the capacitors collecting $Q_1 \sim Q_4$ values have identical response characteristics so that there is no hardware asymmetry error. If such errors are observed, they easily can be removed by swapping capacitors alternately. Following formulations calculate the depth D using $Q_1 \sim Q_4$ and simple trigonometric function induced from the relation illustrated in Fig. 1.

$$\begin{aligned} D &= \frac{c}{2} arctan\left(\frac{Q_3 - Q_4}{Q_1 - Q_2}\right) \\ &= \frac{c}{2} arctan\left(\frac{n\alpha q_3 - n\alpha q_4}{n\alpha q_1 - n\alpha q_2}\right) \\ &= \frac{c}{2} arctan\left(\frac{q_3 - q_4}{q_1 - q_2}\right) \end{aligned} \tag{1}$$

where $c \simeq 3 \times 10^8$ m/s is the speed of light. $Q_1 \sim Q_4$ represent total electric charge values and $q_1 \sim q_4$ represent normalized amount of electric charge values. n is the number of IR signal cycles used for the depth calculation and α is the amplitude of reflected IR that varies along the flying distance and object color. In general, we repeat the calculation n times during the integration time average the calculated depth values to increase signal-to-noise ratio. This means that the sensor expects that the reflected IR signals stay unchanged during the integration time. In normal cases, we can eliminate n and α in the equation (1). In other words, the calculated depth is not dependant upon the number of signal cycles used for the depth calculation and signal amplitude (or object color and flying time). In this normal status, we have two rules that have to be satisfied from their phase offset relations.

$$Q_1 + Q_2 = Q_3 + Q_4 = Q^{sum} \tag{2}$$

$$|Q_1 - Q_2| + |Q_3 - Q_4| = Q^{sum} \tag{3}$$

Let's call equation (2) Plus Rule and equation (3) Minus Rule, respectively. Q^{sum} is the total amount of electric charge that is delivered by reflected IR signal within the integration time. Plus Rule is clear from the Fig. 1. The control signals C_1 and C_2 are alternately turned on with $180°$ phase delay, total collected charge value from both C_1 and C_2 becomes constant. Minus Rule is also can be derived from the fact that the control signals C_3 and C_4 have $90°$ phase delay from the control signals C_1 and C_2, and the sum of absolute differences of both pairs becomes Q^{sum}. This can be rewritten as follows.

$$q_1 + q_2 = q_3 + q_4 = q^{sum} \tag{4}$$

$$|q_1 - q_2| + |q_3 - q_4| = q^{sum} \tag{5}$$

because, $n > 0$ and $\alpha > 0$ in equation (1).

III. Motion Blur Detection

Let's assume that any motion of camera or object occurs during an integration time that changes the phase offsets of the reflected IR signal as indicated in gray color in Fig. 2. Fig. 2 shows what happens if there is any phase mixing due to the motion within the integration time with four-phase (using four control signals $C_1 \sim C_4$ to calculated the depth) time-of-flight sensor. Because ToF sensors calculate depth values n times at n IR signal cycles and average them during the integration time, this phase mixing due to the motion causes wrong depth calculation. Fig. 3 show sample four intensity images consist of respective electric charge values and depth, IR intensity images. In order to collect enough amount of electric charge values $Q_1 \sim Q_4$ for accurate depth calculation, we have to keep at least significant length of integration time. As many consumer ToF depth sensors do, we assume that our depth camera has two storing capacitors and four control signals for depth calculation. In real ToF sensors, it is not possible to turn on any two control signals simultaneously to charge both capacitors altogether. Therefore, C_1 and C_2 can share a capacitor and C_3 and C_4 as well. In this case, different from the conceptual illustration in Fig. 2, only two control signals can collect and store electric charge values simultaneously. Therefore, we have two stages in the integration time (in the graph on the left). During the first half of the integration time Q_1 and Q_2 are collected. Q_3 and Q_4 are collected during the second half of integration time. Let's assume that our sensor calculates depth values n times at n IR signal cycles. In general, we do not know how many times of depth change will occur within the integration time. Let's assume that we have K depth changes. Then the equation (1) can be rewritten as follows.

$$\begin{aligned} D &= \frac{c}{2} arctan\left(\frac{\sum_{i=1}^{K}(m_i\alpha_i\widehat{q_{i3}}) - \sum_{i=1}^{K}(m_i\alpha_i\widehat{q_{i4}})}{\sum_{i=1}^{K}(m_i\alpha_i\widehat{q_{i1}}) - \sum_{i=1}^{K}(m_i\alpha_i\widehat{q_{i2}})}\right) \\ &= \frac{c}{2} arctan\left(\frac{\sum_{i=1}^{K} m_i\alpha_i(\widehat{q_{i3}} - \widehat{q_{i4}})}{\sum_{i=1}^{K} m_i\alpha_i(\widehat{q_{i1}} - \widehat{q_{i2}})}\right) \end{aligned} \tag{6}$$

where $\sum_{i=1}^{K} m_i = n$ and hat notation represents that electric charge is collected when there exist motion blur. From this formulation, we know that n and α are not possible to eliminate any more if there is any motion blur. In other words, the calculated depth in motion blur region depends on the number of cycles used for the depth calculation and IR signal amplitude (or object color and flying time).

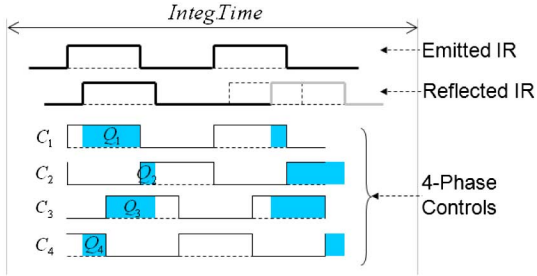

Fig. 2. Phase mixing due to any motion of camera or object.

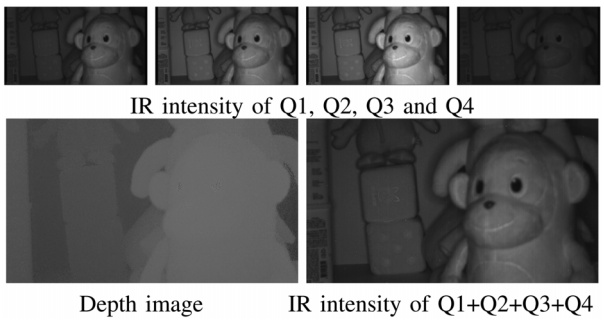

Fig. 3. IR Intensity and Depth Images of Our Prototype ToF Sensor.

Theoretically, our Plus (equation (2)) rule is still valid in this motion blur status.

$$Q_1 + Q_2 = \sum_{i=1}^{K} m_i \alpha_i (\widehat{q_{i1}} + \widehat{q_{i2}}) = \sum_{i=1}^{K} m_i \alpha_i (\widehat{q^{sum}}) = \sum_{i=1}^{K} m_i \alpha_i (\widehat{q_{i3}} + \widehat{q_{i4}}) = Q_3 + Q_4 \quad (7)$$

On the other hand, Minus (equation (3)) rule is not always true in this case, because $|\sum_{i=1}^{K} m_i \alpha_i (\widehat{q_{i1}} - \widehat{q_{i2}})| = \sum_{i=1}^{K} m_i \alpha_i (|\widehat{q_{i1}} - \widehat{q_{i2}}|)$ is not always true. At first stage, Q_1 and Q_2 are charged during $n/2$ cycles and at the next stage Q_3 and Q_4 are charged during another $n/2$ cycles. This changes equation (6) as follows.

$$D = \frac{c}{2} arctan \left(\frac{\sum_{i=\gamma+1}^{K} m_i \alpha_i (\widehat{q_{i3}} - \widehat{q_{i4}})}{\sum_{i=1}^{\gamma} m_i \alpha_i (\widehat{q_{i1}} - \widehat{q_{i2}})} \right) \quad (8)$$

where $\sum_{i=1}^{K} m_i = n$. In this situation, Plus (equation (2)) rule does not work either, because $\sum_{i=1}^{\gamma} m_i \alpha_i (\widehat{q_{i1}} + \widehat{q_{i2}}) \neq \sum_{i=\gamma+1}^{K} m_i \alpha_i (\widehat{q_{i3}} + \widehat{q_{i4}})$. This is a general depth calculation equation with all types of motion blurs. These observations are enough to identify motion blur pixel by just investigating $Q_1 \sim Q_4$ values of the pixel without any additional information from neighbors. For experimental evaluation, we assume that we have single depth change causing motion blur within an integration time; from fronto-parallel foreground to fronto-parallel background or vice versa.

IV. Depth Motion Deblurring

Based on the detected blur pixels, we propose a simple but effective depth image deblurring method. Blur region in depth image looks like a hole that can be inpainted manipulating surrounded pixel information. This is, however, not appropriate in 3-D depth image because it causes too much geometrical distortion. Furthermore state of the art inpainting methods with competitive performance are computationally expensive with complex algorithms to be applied for on-line 3-D applications.

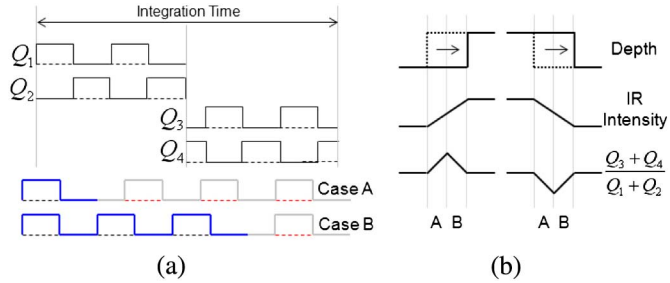

Fig. 4. Phase mixing within an integration time causing a miscalculation of depth.

In order to guarantee the applicability of the proposed deblurring method on real ToF sensors, the following four conditions are considered. 1) It should not use any information from neighbor pixels and performs pixel-wise processing in original depth calculation step 2) and requires minimum additional memory 3) minimum additional processing time with 4) competitive deblurring performance. Let's revisit the principle of ToF depth calculation with square wave IR signal. Fig. 4(a) shows that a phase mixing within an integration time corrupts either Q1 and Q2 (Case A) or Q3 and Q4 (Case B). By investigating the relation between the electric charge values, two cases (A and B) easily can be identified as illustrated on the right of Fig. 4. Following our Plus rule (eq. (4)) $\frac{Q_3+Q_4}{Q_1+Q_2}$ has to be 1 if there is no electronic charge corruption.

In our single depth change assumption, we have to decide which pair of electric charges is distorted by the phase mixing. This can be detected by the following relations. Around the moving objects, phase mixing has two different cases; a phase mixing from longer depth to shorter depth and vice versa. By investigating the slope of IR intensity and the $\frac{Q_3+Q_4}{Q_1+Q_2}$ shown in Fig. 4(b), distorted pair easily can be identified (case A or B). Based on the Plus and Minus Rules (equation (2) and equation (3), respectively), we derive the following equation for each case A and B. Let's investigate the case A first. In the Minus Rule, we know that Q^{sum} is constant and equals to $Q_1 + Q_2$ or $Q_3 + Q_4$. Because Q_1 and Q_2 are corrupted in case A in Fig. 4, we replace Q_1 and Q_2 by uncorrupted Q_3 and Q_4 using the equation ($|Q_1 - Q_2| + |Q_3 - Q_4| = K = Q_1 + Q_2 = Q_3 + Q_4$) according to the distance of target object from the camera. For instance, when $Q_1 > Q_2$ and $Q_3 > Q_4$ (sub-case (a) in Fig. 1), $Q_1 - Q_2 + Q_3 - Q_4$ equals to $Q_1 + Q_2$ and $Q_1 = \frac{Q_3+3Q_4}{2}$ and $Q_2 = \frac{Q_3-Q_4}{2}$ can be obtained. All other sub-cases ((b),(c) and (d) in Fig. 1 along the object distance) are also can be obtained in the similar manner. In the case B in Fig. 4, we replace Q_3 and Q_4 by uncorrupted Q_1 and Q_2. Following this method, we recover depth values of the motion blur pixels. This is very simple but effective and fast deblurring method which is appropriate for hardware implementation without additional memory and processing time.

V. Experimental Results

For the experimental evaluation of the proposed blur detection and deblurring method, we implemented the method in

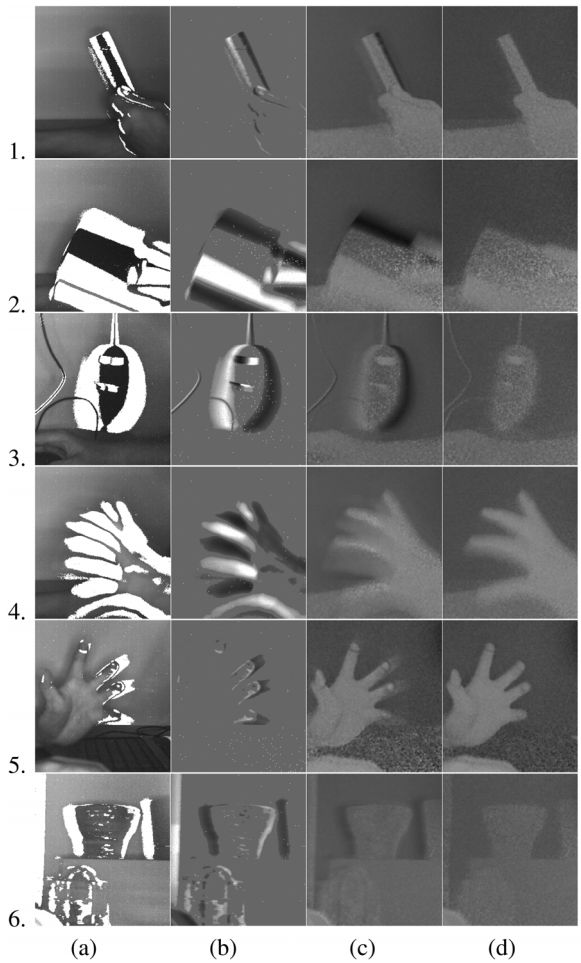

Fig. 5. Depth Deblurring Results: (a) Blur Detection (b) $\frac{Q_3+Q_4}{Q_1+Q_2}$ (c) Input Depth (d) Deblur Result.

our prototype ToF depth sensor [9] working in four-phase and two-capacitor scheme. Sensing range of the camera is 7.5 meters. Fig. 5 summarizes experimental results in various challenging conditions of objects or camera motions. Example 1,2 and 3 are all rigid-object movements. First example has relatively narrow body and moved left and right as detected in the detection result image of the first column (white colored region). Second column images are $\frac{Q_3+Q_4}{Q_1+Q_2}$ values of each pixel that is explained in Fig. 4(b). This value is used to detect the blur region as well as current moving front. As illustrated in Fig. 4(b), darker pixels represent the front side of moving direction of the object. In example 1, we can see that the object is currently moving toward the right direction. Example 2 has relatively thick body and faster movement (wider blur regions). Example 3 shows detected blur regions of a non-flat object. Not just around the object boundary, we also detect the regions on the object surface where a slight depth difference of the object surface causes motion blur. Even very slight motion of the thin electrode lead on the left side of the image is correctly detected. This motion blur region only spans a couple of depth pixels. Our method investigates the validity of the depth calculation at each pixel and detects any single corrupted pixel. Example 4 and 5 are non-rigid objects. Random, complicated and overlapped motions of five fingers in the example 4 are all correctly detected and clearly removed. Deblurring of these

TABLE I
PROCESSING TIME COMPARISON OF BLUR DETECTION AND DEBLURRING

	Post Proc.[1]	Normal Neigh.[3]	**Proposed**
Blur Detection	124.63sec	0.03sec	<0.001sec
Deblurring	NA	11.52sec	<0.001sec

non-rigid human body motions is critical for accurate 3-dimensional interaction with fast moving fingers. Example 5 shows more complicated motion blur including the finger motion along the depth direction that is correctly detected and removed. Example 6 has camera motion with static scene. Different from the previous cases, brighter color in $\frac{Q_3+Q_4}{Q_1+Q_2}$ image (second column in Fig. 5) represents the direction of the camera motion. Motion blur elimination caused by any camera motion is critical when we use consumer depth cameras for 3-dimensional reconstruction moving around the scene. Even though we are assuming a single depth change in our experiments, deblurring performance of the proposed method on some complicated motions are competitive. In reality, multiple and significant depth changes in single pixel within less than hundred millisecond of integration time is rare. Note that the proposed method removes motion blur without losing any detail of original depth image, because the detection and elimination of blur pixels are performed independently without any help or information from neighbour pixels.

VI. CONCLUSION

In this letter, we propose a simple but effective depth motion blur detection and deblurring method based on our thorough analysis on ToF principle with moving observations. We have proved the performance of the proposed method experimentally using our prototype ToF depth sensor with challenging examples. Our method can be easily adapted to any other consumer ToF based depth sensors. Deblurring is critical pre-processing for any application of any research field due to its serious distortions on the observed 3-dimensional geometry. Average processing time of our method can hardly be noticed in any real-time imaging condition (Table I).

REFERENCES

[1] S. Lee, H. Shim, J. D. K. Kim, and C.-Y. Kim, "Tof depth image motion blur detection using 3d blur shape models," in *Proc. SPIE Electron Imag.*, Jan. 2012.
[2] O. Whyte, J. Sivic, A. Zisserman, and J. Ponce, "Non-uniform deblurring for shaken images," in *Proc. IEEE Conf. Computer Vision and Pattern Recognition*, Jun. 2010, pp. 491–498.
[3] S. Lee, B. Kang, J. D. K. Kim, and C.-Y. Kim, "Motion blur-free time-of-flight range sensor," in *Proc. SPIE Electron Imag.*, 2012.
[4] S. Hussmann, A. Hermanski, and T. Edeler, "Real-time motion artifact suppression in tof camera systems," *IEEE Trans. Instrum. Meas.*, pp. 1682–1690, 2011.
[5] O. Lottner, A. Sluiter, K. Hartmann, and W. Weihsm, "Movement artefacts in range images of time-of-flight cameras," in *Int. Symp. Signals, Circuits and Systems*, 2007, pp. 1–4.
[6] M. Lindner and A. Kolb, "Compensation of motion artifacts for time-of-flight cameras," *Dynam. 3D Imag.*, pp. 16–27, 2009.
[7] M. Schmidt and B. Jahne, "Efficient and robust reduction of motion artifacts for 3d time-of-flight cameras," in *Proc. IEEE Int. Conf. 3D Imaging*, 2011, pp. 1–8.
[8] B. Kang, S.-J. Kim, S. Lee, K. Lee, J. D. K. Kim, and C.-Y. Kim, "Harmonic distortion free distance estimation in tof camera," in *Proc. SPIE Electron Imag.*, 2011.
[9] S.-J. Kim, B. Kang, J. D. Kim, K. Lee, C.-Y. Kim, and K. Kim, "A 1920×1080 $3.65\ \mu$m-pixel 2d/3d image sensor with split and binning pixel structure in $0.11\ \mu$m standard cmos," in *Proc. IEEE Int. Solid-State Circuits Conf.*, 2012, pp. 27–29.